

On some developments and evaluation of an Eulerian-Lagrangian method for the transport equation

F. Bierbrauer* W. K. Soh* W. Y. D. Yuen[†]

(Received 7 August 2000)

Abstract

The modelling of typical engineering problems in industry, such as water-jet cooling of hot-rolled steel strip products, directly involves

*Department of Mechanical Engineering, University of Wollongong, Wollongong, NSW 2522, AUSTRALIA. fb01@uow.edu.au and <mailto:wksoh@uow.edu.au>

[†]BHP Steel Research Laboratories, P.O. Box 202, Port Kembla, NSW 2505, AUSTRALIA. <mailto:yuen.daniel.dw@bhp.com.au>

⁰See <http://anziamj.austms.org.au/V42/CTAC99/Bier> for this article and ancillary services, © Austral. Mathematical Soc. 2000. Published 27 Nov 2000.

the solution of a transport (advection-diffusion) equation for the cooling characteristics of the strip. The non-linear nature of the heat conduction involved aggravates the difficulty of the problem.

Traditional Finite Difference techniques for the solution of this advection dominated transport equation incur severe Courant number stability restrictions as well as instabilities in the presence of temperature discontinuities. Eulerian-Lagrangian Methods (ELM's) solve the transport equation in Lagrangian form 'along' backward characteristics effectively decoupling the advection and diffusion terms but retaining the convenience of fixed computational grids. Typical interpolation methods used to obtain the values at the feet of characteristic lines lead to spurious oscillations, numerical diffusion, peak clipping and phase errors.

Through the use of 'peak tracking', by the forward-tracking of Eulerian nodal points, this paper attempts to alleviate these errors. A comparison of 1-D benchmark tests from the Convection-Diffusion Forum as well as appropriate error measures, are shown to produce appreciable improvements over the standard methods for a range of time steps, very large Peclet numbers and Courant numbers in excess of one.

Contents

1 Introduction	C240
2 Eulerian-Lagrangian Method	C245
2.1 Numerical Formulation of the ELM	C246
3 Benchmark Tests	C251
4 Summary and Conclusions	C254
References	C259

1 Introduction

Industrial problems involving the solution of the advection-diffusion/transport equation range from the solution of fluid dynamical problems such as the galvanisation of steel sheets and alloy solidification, to heat transfer applications such as the temperature increase in current carrying wires [2] and the water jet cooling of a moving hot rolled steel strip [13]. The latter problem, currently under investigation by the authors, involves not only a transport equation for the strip temperature distribution but also non-linear temperature boundary conditions due to nucleate boiling heat transfer on the surface of the strip and discontinuous temperature jumps at the jet impact site [13].

Traditionally, purely Eulerian numerical techniques, such as Finite Difference Methods (FDM), applied to such a problem lead to severe Courant number stability restrictions. As well, these methods suffer from unphysical spatial oscillations for Peclet numbers greater than two [8]. Upwinding methods, used to retard these oscillations through artificial diffusion, require at least third-order upwinding and lead to non-tridiagonal matrices [6] often requiring long solution times, are still Courant number dependent [6] and fail to be Galilean invariant in higher dimensions.

On the other hand purely Lagrangian methods deal admirably with advection but are made unattractive due to practical difficulties such as grid deformation in the presence of complex flows [10].

‘Eulerian-Lagrangian methods (ELM)’ effectively decouple the advective and diffusive terms by splitting the transport processes, first solving a purely hyperbolic advective equation using a Lagrangian technique which follows the flow along characteristic lines, followed by the solution of a purely parabolic diffusion equation on an Eulerian grid [12, 10, 11]. Previous research has shown that this strategy eliminates Courant number restrictions and handles processes possessing significantly different time scales [5]. Most FD-ELM’s may be classified as one of two methods: ‘interpolation ELM’s’ and ‘piecewise integration ELM’s’ with other types such as ‘Quadrature Finite Element Methods (FE-ELM’s)’ and ‘Eulerian-Lagrangian localised adjoint methods’ (ELLAM) being specific to FE-ELM’s, here we use the nomenclature of de Oliveira [10].

The generic steps inherent to ELM's include (i) a way to track the characteristic lines (to either the 'head' \equiv next time level or 'feet' \equiv previous time level, of the line) followed by (ii) the determination of the Lagrangian values at the feet of the characteristic lines and finally (iii) the solution of the Lagrangian form of the diffusion equation using the values obtained in (ii) as initial conditions [11, 14]. While the forward-tracking of characteristic lines using fictitious particles has been pursued by some researchers [7], it suffers from instabilities at larger time steps. In general, a combination of single time step, reverse, fictitious particle tracking (SRPT) [3] and some sort of forward particle node tracking (FPT) is used by most researchers [12, 9, 11, 14]. In general, the backward-tracked foot of the characteristic line will not coincide with the fixed Eulerian nodes so that interpolation from either neighbouring nodes and/or forward-tracked nodes must be used to obtain Lagrangian values.

De Oliveira & Baptista [12] have shown that tracking errors contribute to mass conservation and phase errors, as well as leading to both negative and positive numerical diffusion which generate instability and accuracy problems respectively [12]. Inaccurate interpolation at the feet of characteristic lines leads to mass errors [12] and the order determines the stability, numerical diffusion and spurious oscillations present in the method [14]. The seminal research of Yeh et al [14] has shown that peak clipping and valley elevating are the most important factors generating numerical diffusion, spurious oscillations and phase errors [14].

Using a combination of SRPT, continuous (C)FPT and fourth order Runge-

Kutta-Fehlberg tracking, Neuman [9] avoided numerical diffusion, peak clipping, spurious oscillations and accurately modelled 1-D ‘Gaussian hills’ and advancing fronts for Peclet numbers from zero to infinity and Courant numbers greater than one. The need to compensate for diffusion for continuously forward-tracked particles was avoided by the projection of new time data to the particles at each time step. This method resolves many problems but relies on a large number of particles in the vicinity of high curvature regions and must keep track of them continuously throughout the calculation.

The ‘interpolation ELM’ of Casulli [3] and Cheng et al used a SRPT with one step and multi-step Euler [3] tracking and second order Lagrangian polynomials to determine the backward-tracked values for 1-D and 2-D problems. Some mass and phase errors resulted and sharp front changes could not be adequately resolved.

Building on the initial concepts of Neuman [9], Yeh et al [14] constructed a ‘piecewise integration method’ using a zoomable and adaptable hidden fine-mesh approach which not only uses SRPT and CFPT but also assigns ‘notable points’ in regions of extreme curvature. The structure of the hidden mesh points is automated and allows calculation to within the required tolerance for exact peak capturing and eliminates spurious oscillations, numerical diffusion and phase errors. Care must be taken with forward-tracked points to ensure they ‘diffuse’ correspondingly as the calculation is stepped forward in time. This is provided by a compensation factor [14] after the solution of the diffusion equation. Yeh et al [14] reported very high accuracy with 1-D benchmark problems although the extension to higher dimensions appears

problematic. Very high computational costs, related to the accumulating number of necessary notable points, provide a disincentive for its use.

A much simpler ‘piecewise integration method’ related to that of Yeh et al [14] (SRPT, linear polynomials for backward-tracked values with 5th order Runga-Kutta tracking) using single time step FPT (SFPT) from Eulerian nodal points, for the initial conditions for the diffusion step about a ‘core element’ in the neighbourhood of the feet of characteristic lines, was developed by de Oliveira [10]. This method is natural to FE-ELM’s not being directly amenable to FD-ELM’s. It does not possess notable points thereby reducing the high computational costs inherent to Yeh’s method, and the correction of forward-tracked nodes is eliminated [10].

The current ‘interpolation FD-ELM’ attempts to alleviate these problems, as well as simplifying the method as much as possible. Using an FD-ELM defined in Section 2, with both SRPT and SFPT for backward and forward-tracked points, Section 2.1 Part 1, Lagrangian values are obtained by using four point Lagrangian polynomials, Section 2.1 Part 2, as interpolators at backward-tracked points. Time and memory considerations are reduced through lower storage requirements and the use of an iterative Successive Overrelaxation scheme (SOR), in Section 2.1 Part 3, for the solution of the diffusion equation. The main aim of this paper is to solve the transport equation with the most simplified ELM treatment possible, that is, an ‘interpolation FD-ELM’ with SR/FPT and iterative diffusion equation solver. The method is directly extendable to an FE-ELM with its accompanying advantages as well as improvements in peak tracking through CFPT with diffusive

compensation factors without piecewise integration.

In Section 3 numerical tests of the method conducted with the use of ‘Gaussian hill’ 1-D benchmarks, available from the Convection-Diffusion Forum [1], are used to test the accuracy and adaptability of the current ELM. Formal error measures examine the accuracy of the method for a variety of Courant and Peclet numbers and a range of timesteps. Section 4 reviews the results, discusses the further development of the method and the implications for future research directions.

2 Eulerian-Lagrangian Method

Consider the Lagrangian operator version of the 1-D transport equation in the domain $\Omega = \{x \in \mathbb{R}, t > 0\}$:

$$\frac{DC}{Dt} = \alpha \frac{\partial^2 C}{\partial x^2} \quad (1)$$

where the co-moving derivative D/Dt indicates the time rate of change is calculated along a characteristic line defined by the solution of:

$$\frac{dx}{dt} = u(x, t) \quad (2)$$

and

$$\frac{D}{Dt} \equiv \frac{\partial}{\partial t} + u(x, t) \frac{\partial}{\partial x}$$

where C is the appropriate variable such as concentration, x is the space dimension, t time, α a known constant (diffusion coefficient) and $u(x, t)$ the given velocity field. The equation is solved subject to the initial and boundary conditions:

$$C(x, 0) = C_0(x)$$

$$C|_{\partial\Omega} = f(t)$$

where $\partial\Omega$ is the boundary and $C_0(x)$ and $f(t)$ are prescribed functions.

2.1 Numerical Formulation of the ELM

We discretise the above domain with fixed Eulerian nodes defined by $x_i = i\Delta x$, $i = \{0, 1, 2, \dots, I\}$ and time given by $t^n = n\Delta t$, $n = \{0, 1, \dots\}$, where Δx is selected for the particular benchmark problem and Δt is determined as a multiple of the advective time step $\Delta t = \Delta x/u$. This is clearly shown in Figure 1. Adopting the notation of Neuman [9] the Crandall method of weighted averages [4], is defined by:

$$\frac{C_i^{n+1} - C_{i-c_u}^n}{\Delta t} = \alpha\theta \left[\frac{\partial^2 C}{\partial x^2} \right]_i^{n+1} + \alpha(1 - \theta) \left[\frac{\partial^2 C}{\partial x^2} \right]_{i-c_u}^n \quad (3)$$

and

$$\left. \frac{\partial^2 C}{\partial x^2} \right|_i = \frac{C_{i+1} - 2C_i + C_{i-1}}{\Delta x^2}, \quad \left. \frac{\partial^2 C}{\partial x^2} \right|_{i-c_u} = \frac{C_{i-c_u+1} - 2C_{i-c_u} + C_{i-c_u-1}}{\Delta x^2}$$

where for example $\theta = 1, 1/2, 0$, the time weighting factor ($0 < \theta < 1$), represents a purely implicit, Crank-Nicolson type semi-implicit method and explicit method respectively. Here, $Cu_i^n = u_i^n \Delta t / \Delta x$ is the grid Courant number which is, in general, not an integer and may be space and time dependent. Thus the backward-tracked point at time t^n , $x_{bt} = (i - Cu)\Delta x$, which lies on the characteristic line passing through the point $x_i = i\Delta x$ at time t^{n+1} , is not a grid point (unless Cu is an integer) and an interpolation formula must be used to construct the value C_{i-Cu}^n which remains constant along the characteristic line (2).

The three steps underlying ELM's are:

1. *Definition and location of heads and feet of characteristic lines*

At any time t^n the solution of the hyperbolic equation in Lagrangian form is carried out by backward-tracking fictitious particles along the characteristic line passing through the Eulerian nodes $x_i = i\Delta x$ at time t^{n+1} until the foot, $x_{bt}^n = (i - Cu)\Delta x$, of the characteristic line is reached at t^n , open circles in Figure 1. In order to reduce peak clipping and other problems, fictitious particles are forward-tracked along the characteristic line passing through Eulerian nodes $x_i = i\Delta x$ at time t^{n-1} until the head, $x_{ft}^n = (i + Cu)\Delta x$, is reached at t^n , circles with central dots in Figure 1. These backward and forward-tracked points at time t^n are located by solving the characteristic equation (2) backwards

or forwards in time respectively. That is:

$$x_{bt}^n = x_i^{n+1} - \int_{t^n}^{t^{n+1}} u(x_i, t^{n+1}) dt \quad (4)$$

for the backward-tracked point and

$$x_{ft}^n = x_i^{n-1} + \int_{t^{n-1}}^{t^n} u(x_i, t^{n-1}) dt \quad (5)$$

for the forward-tracked point. The calculation of these integrals is carried out by a second order Runge-Kutta (RK) method [12].

2. Determination of concentrations at feet of characteristic lines

At time t^n the backward-tracked concentrations, $C_{i-C_u}^n = C^n(x_{bt})$, may be constructed by Lagrangian polynomial interpolation from nearby given Eulerian nodal points, $C_i^n = C^n(x_i)$, and forward-tracked concentrations, $C_{i+C_u}^{n-1} = C^{n-1}(x_{ft})$, defined by:

$$C_{i-C_u}^m = \sum_{j=1}^J \left[\prod_{k=1(\neq j)}^J \left(\frac{x_{bt} - x_k}{x_j - x_k} \right) \right] C_j$$

where $x_j = \{\dots, x_i^n, \dots; \dots, x_{i+C_u}^n, \dots\}$,

$C_j = \{\dots, C_i^n, \dots; \dots, C_{i+C_u}^{n-1}, \dots\}$

and $j = \{1, 2, \dots, \text{degree of polynomial}\}$.

3. *Solution of Lagrangian form of diffusion equation with values of 2. as initial conditions*

The backward-tracked concentrations, C_{i-Cu}^n , are used as initial conditions in the solution of (1) via a SOR scheme defined by:

$$C_i^{k+1} = C_i^k + \lambda(C_i^{(*)} - C_i^k) \quad (6)$$

where the solution $C_i^{(*)}$ is combined with the previous solution C_i^k

$$(1 + 2s)C_i^{(*)} = s(C_{i+1}^k + C_{i-1}^{k+1}) + C_{i-Cu}^k \quad (7)$$

$$(1 + 2s)C_i^{k+1} = s(C_{i+1}^k + C_{i-1}^k) + C_{i-Cu}^k \quad (8)$$

in the purely implicit case and an analogous definition for the semi-implicit case. Here, k is the iteration parameter, λ the relaxation parameter ($0 < \lambda < 2$) and $s = \alpha\Delta t/\Delta x^2 = Cu/Pe$, $Pe = u\Delta x/\alpha$ (Peclet number). The stopping criterion is chosen such that

$$|C^{k+1} - C^k| \leq \text{tolerance}$$

where the tolerance is selected beforehand.

Note that the Courant number may be split into integer and fractional parts:

$$Cu_{int} = \text{int}(Cu), \quad Cu_{fr} = Cu - Cu_{int}$$

If $Cu_{fr} = 0$ then any backward-tracked point coincides with an Eulerian node and no information is lost resulting in an exact solution of the transport

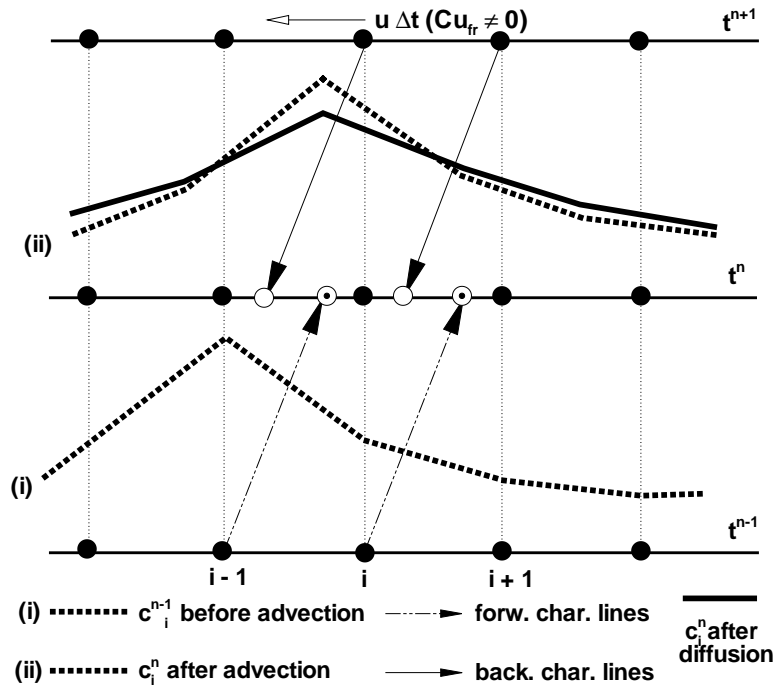


FIGURE 1: The three steps of the ELM proposed by the authors.

equation. Selection of such time steps is not always possible and artificially restricts the usefulness of the ELM. Note that it is possible to construct an ELM with notable points using interpolation to determine backward-tracked values (ie not a piecewise function as in Yeh [14]) by recalculating the value of continuously forward-tracked points through the diffusive term αC_{xx} which may be constructed from Taylor series approximations of nearby nodes even if the nodes are unevenly distributed.

3 Benchmark Tests

To study the efficacy of the current ELM we choose a 1-D benchmark test from the CD forum [1]. The transport of a ‘Gaussian concentration hill’ in uniform flow:

$$\frac{\partial C}{\partial t} + u \frac{\partial C}{\partial x} = \alpha \frac{\partial^2 C}{\partial x^2} \quad -\infty < x < \infty$$

$$C(x, 0) = C_0(x), \quad C(x, t) = 0 \text{ as } |x| \rightarrow \infty$$

with the solution

$$C(x, t) = \left(\frac{\sigma_0}{\sigma} \right) \exp \left(-\frac{(x - \bar{x})^2}{2\sigma^2} \right)$$

where

$$\sigma = \sqrt{\sigma_0^2 + 2\alpha t} \quad \bar{x} = x_0 + \int_0^t u(x, t') dt'$$

u is now a Lagrangian variable. In order to measure the accumulation of error we make use of the error measures defined in the CD forum [1] and de Oliveira & Baptista [12]: measures of mass conservation, ability to preserve peaks, artificial spreading of the numerical solution, phase shift and L_2 error. These are defined by: Measure of global mass

$$m_{err}(t) = \frac{1}{m_{ex}(t)} \int_{\Omega} C_{num}(x, t) dx$$

Discrete L_2 -norm

$$L_2(t) = \frac{1}{m_{ex}(t)} \int_{\Omega} [C_{num}(x, t) - C_{ex}(x, t)]^2 dx$$

Integral measure of phase shift

$$\mu_x(t) = 1 - \frac{\frac{\int_{\Omega} x C_{ex} dx}{m_{ex} t} - \frac{\int_{\Omega} x C_{num} dx}{m_{num} t}}{\Delta x}$$

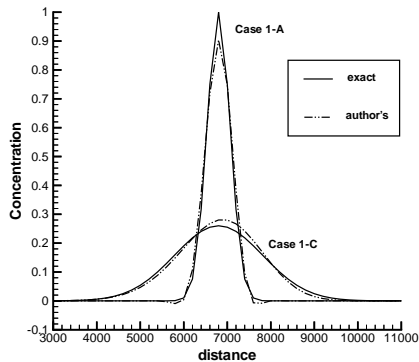
Integral measure of numerical diffusion

$$\mu_{xx}(t) = \frac{\int_{\Omega} \left[x - \frac{\int_{\Omega} x C_{num} dx}{m_{num}} \right]^2 C_{num} dx}{\int_{\Omega} \left[x - \frac{\int_{\Omega} x C_{ex} dx}{m_{ex}} \right]^2 C_{ex} dx} \frac{m_{ex}(t)}{m_{num}(t)}$$

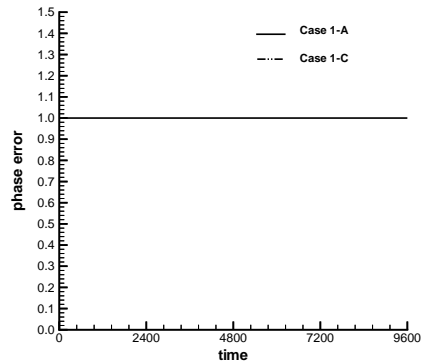
We consider two time steps: $\Delta t < \Delta x/u$ and $\Delta t > \Delta x/u$, the case $\Delta t = \Delta x/u$ results in exact solutions since $Cu_{fr} = 0$. For each of these two time steps we selected the transport of a ‘Gaussian hill’, Cases 1-A and 1-C, used in the CD forum [1], see Table 1.

TABLE 1: Time step and Case data for Gaussian hill benchmark tests

time step	no. steps	Case	Δx	u	σ	α	Cu	Pe	$\frac{Cu}{Pe}$
$\Delta t < \frac{\Delta x}{u} = 96$	100	1-A	200	0.5	264	0	0.24	∞	0
		1-C	200	0.5	264	50	0.24	2	0.12
$\Delta t > \frac{\Delta x}{u} = 480$	20	1-A	200	0.5	264	0	1.2	∞	0
		1-C	200	0.5	264	50	1.2	2	0.6

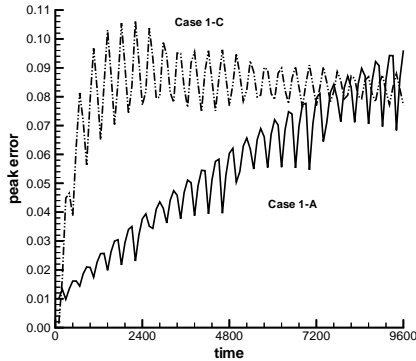


(a)

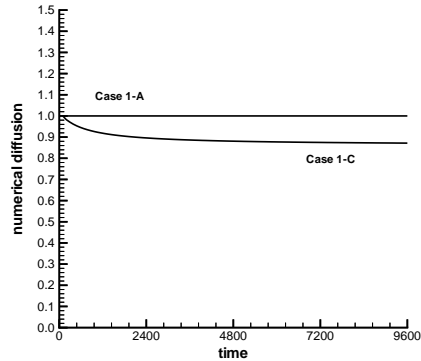


(b)

FIGURE 2: Comparison of Cases 1-A and 1-C with $\Delta t < \frac{\Delta x}{u}$ after 100 time steps: (a) Convection profiles; (b) phase shift;



(c)



(d)

FIGURE 2: (c) peak clipping error; (d) numerical diffusion;

4 Summary and Conclusions

The results are shown in Figures 2 ($\Delta t < \frac{\Delta x}{u}$) and 3 ($\Delta t > \frac{\Delta x}{u}$)

1. $\Delta t < \frac{\Delta x}{u}$: A Comparison of numerical and exact solutions: Figure 2(a) shows good tracking behaviour even for low order RK methods and provides a good qualitative feel for other errors, both low and high diffusion results are quite accurate even for small time steps. Both the global mass, Figure 2(f), and phase errors, Figure 2(b), are minimal although some numerical diffusive error persists when $\alpha \neq 0$. The L_2 -norm, Figure 2(e), shows increasing error for the purely advective case

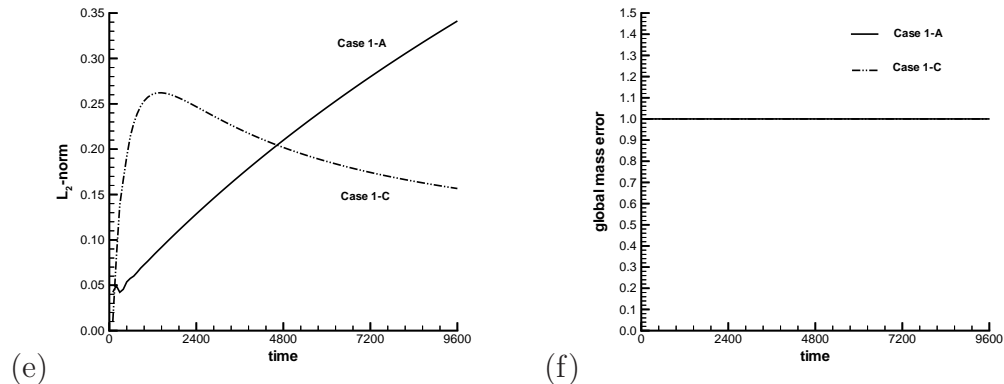
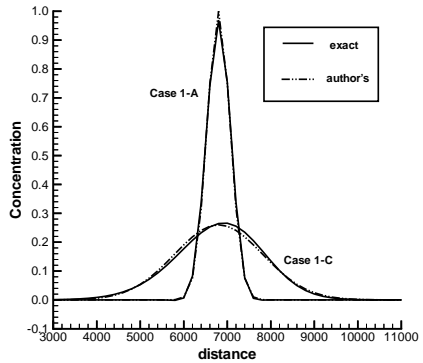


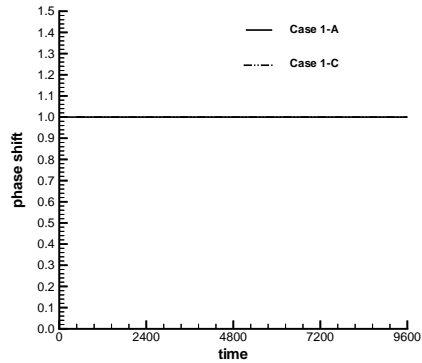
FIGURE 2: (e) Discrete L_2 -norm; (f) global mass error.

although it starts to level out at later time steps, on the other hand the diffusive case appears to reach an average constant value. It seems that the dependence of the peak clipping error, Fig 2(c), rests with the initial time step for the diffusive case and levels out for the advective case. De Oliveira & Baptista [12] have shown that even moderate tracking errors for low order methods can lead to strong error growth, no doubt contributing to the inaccuracies shown in Figure 2.

2. $\Delta t > \frac{\Delta x}{u}$: A study of Figure 3 on the other hand shows that an increase in Δt above the critical value $\Delta x/u$ (corresponding to $Cu = 1$) greatly improves the results with very small errors visible in Figures 3(a,b,d,f) although a very small mass error exists, Figure 3(f). A comparison of



(a)



(b)

FIGURE 3: Comparison of Cases 1-A and 1-C with $\Delta t > \frac{\Delta x}{u}$ after 20 time steps: (a) Convection profiles; (b) phase shift;

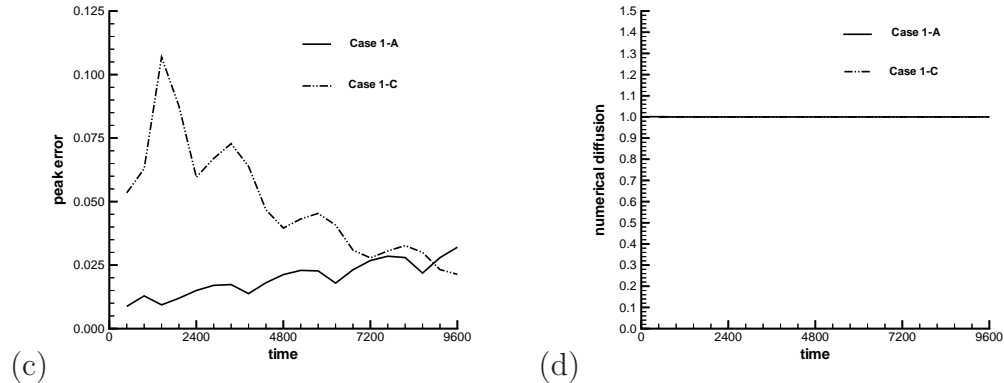


FIGURE 3: (c) peak clipping error; (d) numerical diffusion;

the error present in the two methods, 1-A with 100 time steps and 1-C with 20, is possible by observing each method for the same number of timesteps, ie $n = 20$ or at $t = 1920$ for 1-A and $t = 9600$ for 1-C. 1-C shows considerably better behaviour at $n = 20$. Both the peak and L_2 -norm show excellent behaviour over time without the error increasing greatly beyond a certain value.

No instabilities are present in either of the two cases above even for Courant numbers in excess of one and very high Peclet numbers. The present paper has shown that

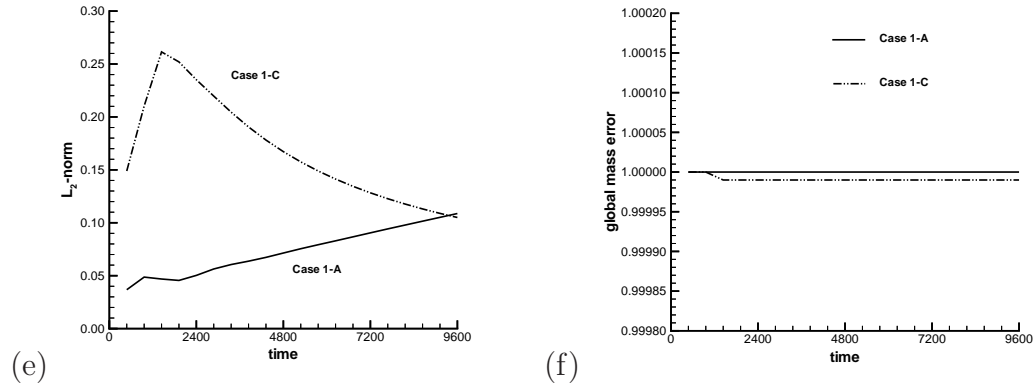


FIGURE 3: (e) Discrete L_2 -norm; (f) global mass error.

- 1-D ‘Gaussian hill’ numerical tests have shown the present simplified ELM to be an accurate, stable and adaptable method for solving the transport equation with excellent Courant and Peclet number characteristics possessing even better behaviour for large time steps, a crucial hindrance in other explicit and implicit FDM’s such as upwinding methods.
- The method, like that of de Oliveira [10], provides a straightforward solution of the transport equation without resorting to notable points with their accompanying high computational costs, complex particle density distributions, ‘diffusion’ compensation factors, seemingly artificial ‘core elements’ and restriction to FE-ELM’s. In addition the

method is extendable to an FE-ELM with its grid structure advantages. Its speed is assured through the straightforward use of an SOR method rather than the far more laborious matrix solvers which cannot be avoided for implicit upwinding FDM's.

3. The present work is only preliminary but provides a guide for further research such as the quantitative stability properties of the ELM: variation with Cu , Pe and $u(x, t)$, accuracy analysis for Lagrange polynomials of higher/lower degree (linear, quadratic etc), effect of Cu_{fr} , effects of tracking errors, stability and accuracy effects of varying concentration boundary conditions, eg: non-linear, non-local, discontinuous. The extension of this method to the solution of the fully non-linear Navier-Stokes equations is a further target and has been shown to be possible by other ELM's such as Neuman's [9]. Previous tests by the authors have shown the ability of the method to handle complex boundary conditions in higher dimensions and for non-constant velocity fields. The further study of these aspects are the aim for the foreseeable future.

Acknowledgements: This work is supported by a Strategic Partnership with the Industry - Research & Training Scheme of the Australian Research Council and BHP Steel Research Laboratories.

References

- [1] A. M. Baptista, E. E. Adams., and P. Gresho. Benchmarks for the Transport equation: The convection-diffusion forum and beyond. In Lynch and Davies, editors, *Quantitative Skill Assessment for Coastal Ocean Models, AGU Coastal and Estuarine Studies*, 47:241–268, 1995. [C245](#), [C251](#), [C252](#), [C252](#)
- [2] V. Bubanja. The AC-DC difference of single junction thermal converters. Submitted. [C240](#)
- [3] V. Casulli, and R. T. Cheng. Semi-implicit finite difference methods for three-dimensional shallow water flow. *Int. J. Numer. Methods Fluids*, 15:629–648, 1992. [C242](#), [C243](#), [C243](#)
- [4] S. H. Crandall. An optimal recurrence formula for the heat conduction equation. *Q. Appl. Math.*, 13:318–320, 1955. [C246](#)
- [5] O. Daubert. Programme HYP1. Rapport C41/74/12, Laboratoire National d’Hydraulique, Chatou, 1974. [C241](#)
- [6] C. A. J. Fletcher. *Computational Techniques for Fluid Dynamics, Vol 1*. Springer, Berlin, 1999. [C241](#), [C241](#)
- [7] A. O. Garder, D. W. Peaceman, and A. L. Pozzi. Numerical calculations of multidimensional miscible displacement by the method of characteristics. *Soc. Petrol. Eng. J.*, 4:26–36, 1964. [C242](#)
- [8] B. P. Leonard. A survey of finite differences with upwinding for numerical modelling of the incompressible convective diffusion equation. In C. Taylor and K. Morga, editors, *Computational*

Techniques in Transient and Turbulent Flow, Vol 2, Recent Advances in Numerical Methods in Fluids, pages 1–35, 1981. Pineridge Press.

C241

- [9] S. P. Neuman. Adaptive Eulerian-Lagrangian finite element method for advection-dispersion. *Int. J. Numer. Methods Eng.*, 20:321–337, 1984. C242, C243, C243, C246, C259
- [10] A. de Oliveira. *A Comparison of Eulerian-Lagrangian Methods for the Solution of the Transport Equation*. MSc Thesis, Oregon Inst. of Science & Technology, Portland, Oregon, 1994. C241, C241, C241, C244, C244, C258
- [11] A. de Oliveira and A. M. Baptista. A comparison of integration and interpolation Eulerian-Lagrangian methods. *Int. J. Numer. Methods Fluids*, 21:183–204, 1995. C241, C242, C242
- [12] A. de Oliveira and A. M. Baptista. On the role of tracking on Eulerian-Lagrangian solutions of the transport equation. *Adv. Water Resour.*, 21:539–554, 1998. C241, C242, C242, C242, C242, C248, C252, C255
- [13] W. K. Soh and W. Y. D. Yuen. Flow visualisation of the boiling heat transfer at the run-out table. In *41st Mechanical Working and Steel Processing Conference, The Iron and Steel Society*, Baltimore, 697–705, 1999. C240, C240
- [14] G. T. Yeh, J. R. Chang, and T. E. Short. An exact peak capturing and oscillation-free scheme to solve advection-dispersion transport

equations. *Water Resour. Res.*, 28:2937–2951, 1992. C242, C242,
C242, C242, C242, C243, C243, C243, C243, C244, C251